



มหาวิทยาลัยนเรศวร
Naresuan University

Print ISSN: 0858-7418
EISSN: 2539-553X

วารสารมหาวิทยาลัยนเรศวร : วิทยาศาสตร์และเทคโนโลยี
Naresuan University Journal

Science and Technology

Volume 26, No.4, October - December 2018

Editor-in-Chief
Prof. Paisarn Muneesawang Ph. D.

NUJST



Preparation and Characterizations of Hydroxyapatite Substituted Boron Cement

Piyanan Boonphayak*, Sirikarn Khansumled, Adisorn Pinmanee and Supakit Phromduang

Department of Industrial Engineering, Engineering Faculty, Naresuan University, Phitsanulok, 65000, Thailand

* Corresponding author. E-mail address: piyananb@nu.ac.th

Abstract

The aim of this research is studying the produce boron substitution into hydroxyapatite (20BHA) cement powder and investigate the effect of citric acid on the compressive strength of new cement. 20BHA cement powder was synthesized by the co-precipitation method at room temperature. Phase and chemical structure of 20BHA powder were confirmed by X-ray diffraction (XRD) and Fourier transform infrared spectroscopy (FT-IR). The morphology in the cements was confirmed by scanning electron microscope (SEM). The effects of adding citric acid to 20BHA powder was found to have a significant effect on the compressive strength properties of cement. Increasing the concentration of citric acid in 20BHA powder was found to have an effect on the large compressive strength.

Keywords: Bioceramics, Hydroxyapatite substitution, Boronhydroxyapatite, Boron, Citric acid

Introduction

Bioceramics are based on calcium phosphate compounds, used as biomaterial because of it has excellent osteoconductive, bioactive properties, non-toxic and no rejection from the human body. Hydroxyapatite ($\text{Ca}_{10}(\text{PO}_4)_6(\text{OH})_2$: HA) is one of the most calcium phosphate compounds which widely used as medical application. Bone cement is one of the most of HA medical application. Bone cement is a substance or component used to heal or repair broken bone for reduced the time and minimally invasive surgery (Ginebra, 2009). There are two types of materials, polymethyl methacrylate (PMMA) (Arora, 2013; Magnan et al., 2013) and calcium phosphate compounds (Ambard & Mueninghoff, 2006; Xu et al., 2017). PMMA has high temperature during setting (Sun, Kwok, & Nguyen, 2006), these is cause to damage a surrounding tissue. Calcium phosphate has lower setting temperature than PMMA, however it has poor the mechanical properties than PMMA. Many researchers studied to improve the mechanical properties of calcium phosphate bone cement (Zhang et al., 2011; Safronova et al., 2009; Pattanayak et al., 2005). The substitution is one of the most to the improvement the their properties (Nabiyouni, Ren, & Bhaduri, 2015; Ratnayake, Mucalo, & Dias, 2017). The HA substituted can occur in Ca site (Cation substitution) and PO_4 and OH site (Anionic substitution) (Pan & Fleet, 2002; Ternane et al., 2002; Šupová, 2015)

- Cation substitution such as Sr^{2+} , Mg^{2+} , Ce^{3+} , Eu^{3+} etc.
- Anionic substitution such as Cl^- , F^- , CO_3^{2-} , SO_4^{2-} etc.

Boron (B) is a member of the group III and it is only one nonmetal. Boron is the element that has so many biological properties as bone metabolism, calcium and bone balance, prevent osteoporosis (Larsson & Fazzalari, 2014; Kolmas et al., 2017) and also, fast healing (Yılmaz & Evis, 2016).

In this study, we present the synthesis hydroxyapatite substituted with boron (20BHA) via co-precipitation method and characterization of 20BHA when occurred the borate substitution into HA structure. Then we also, investigate the effect of citric acid on the compressive strength of 20BHA cement.



Methods and Materials

Synthesis of hydroxyapatite substituted with boron: 20BHA

The 20BHA powder was prepared by co-precipitation method at low temperature (room temperature). The raw materials were maintained the experimental ratio of Ca/P or Ca/(P+B) of 1.67. A mixture of 10 mole of calcium hydroxide 98+% (Acros), 5.4 mole of orthophosphoric acid 85% RPE-ACS (Carlo) and 0.6 mole of boric anhydride (Sigma – Aldrich) were stirred for 12 h. The 20BHA powder was filtered and then dried at 100°C for 24 h. The cement powder was crushed with mortar and passed through a 325 µm sieve. The 20BHA powder was characterized the phase and chemical structure by XRD and FT-IR techniques.

The crystalline structure of 20BHA powder was determined by X-ray Diffraction (XRD) using Philips: X'pert diffractometer, the powder was analyzed with Cu-K α radiation ($\lambda = 1.5406$ nm) produced at 40 kV. The powder was measured the properties by XRD analysis program (Panalytical/Expert 2Theta). The data corrected from $2\theta = 10-60^\circ$. The XRD result was compared to Joint Committee Powder Diffraction Standard (JCPDS). The lattice parameters of hydroxyapatite a- and c-axis (Å) for hexagonal structure were calculated from peak (0 0 2) and (2 2 2), respectively by using equation 1 (Cullity, 1978)

$$\frac{1}{d^2} = \frac{4}{3} \cdot \left(\frac{h^2 + h \cdot k + k^2}{a^2} \right) + \frac{l^2}{c^2} \quad (1)$$

where d is distance (Å) between adjacent planes in the set of Miller indices (h k l).

The percentage of crystallinity (%X_c) for sample was identified using the equation 2;

$$\%X_c = \frac{I_{300} - V_{112/300}}{I_{300}} \cdot 100 \quad (2)$$

Where, I₃₀₀ is intensity of (3 0 0) diffraction peak and V_{112/300} is the intensity of the trough between (112) and (300) reflections, which completely disappears in noncrystalline samples (Landi, Tampieri, Celotti, & Sprio, 2000).

The middle infrared spectroscopy (FT-IR) was used to study the chemical structure that obtains in material, the cement powder was analyzed by Attenuated Total Reflection (ATR) mode and the spectra recorded by Nicolet 6700 in the range 400–4000 cm⁻¹ with a resolution of 5 cm⁻¹.

Cement characterization

20BHA powder was mixed with setting solution for a cement application. In this case, we used the citric acid in different concentrations, 0%, 10% and 20% were studied and using the liquid/powder ratio (L/P ratio) of 0.8 ml/g. The mixture was transferred to molds and cured at room temperature. The specimens were performed with cylindrical dimensions; 6 mm in diameter and 12 mm in height. All specimens were incubated at the room temperature for 21 days. Compressive strength was determined according to American Standard Test Method (ASTM F451-9a) (ASTM 1999) by the Universal Testing Machine (UTM) at room temperature with 5 kN load cell a crosshead speed of 1.0 mm/min and replicated 5 pieces/sample. All specimens were determined the phase transform by XRD. The morphology of specimens were observed by SEM (QUANTA 450, FEI, USA) at magnification 10,000x.



Results

Synthesis and characterization of 2OBHA powder

The phase composition analysis was determined by X-ray diffraction (XRD). Data was identified with reference to Joint Committee on Powder Diffraction Standards (JCPDS) files. From Figure 1 show the XRD pattern of 2OBHA powder was found phase similar to synthetic HA ($\text{Ca}_{10}(\text{PO}_4)_6(\text{OH})_2$) of JCPDS number 74-0565. In addition, the pattern showed broadened peak and inconsiderably separated to each other, providing the low crystallinity degree in powder (Kolmas et al., 2017).

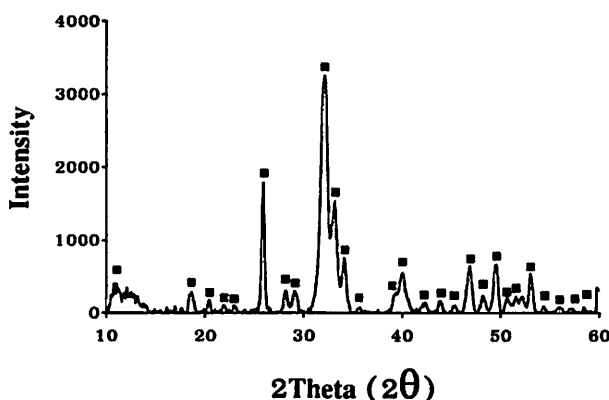


Figure 1 XRD pattern of 2OBHA. Sample was dried at 100°C for overnight. ■ JCPDS number 74-0565.

Table 1 Lattice parameter (a and c), unit cell volume and Crystallinity (%X_c), and of HA synthetic (HA syn) and 2OBHA

Samples	Lattice Parameter		Unit Cell Volume	%Crystalline
	a	c		
HA syn	9.3978	6.8930	527.22	60.91
2OBHA	9.3533	6.8536	519.26	55.42

Table 1 shows that both of unit cell volume and %crystallinity of 2OBHA are decreased with the addition of B³⁺ in the HA structure, due to the ionic radius of the B³⁺ (90 pm) being smaller in size than P³⁺ (110pm) these is result to decreased both of unit cell volume and %crystallinity.

The FT-IR spectra of the 2OBHA sample is shown in Figure 2. It was found that the peak at 2864 cm⁻¹ to 3697 cm⁻¹ and at 1657.11 cm⁻¹ assigned to OH⁻ group and a broad peak at 1424.05 – 1480.82 cm⁻¹ is assigned to C-O stretching of CO₃²⁻ (Fleet, 2009). The peak at 1226.85 cm⁻¹ and 757.74 cm⁻¹ are represented a borate group (BO₃²⁻) (Temane et al., 2002) at 1011.72 cm⁻¹ and 467.91 cm⁻¹– 605.36 cm⁻¹ of the peak assigned to P-O bend PO₄³⁻.

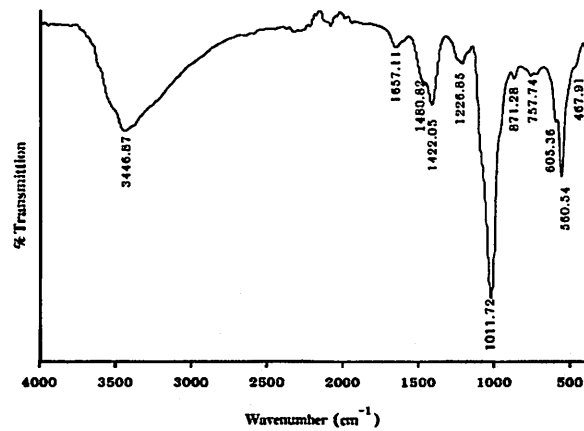


Figure 2 The IR spectra of 20BHA powder was synthesized by Co-precipitation method and dried at 100°C overnight.

From the XRD results (Figure 1) we cannot identified the substitution of borate in HA structure, but the borate substituted replace phosphate group in HA structure shown in FT-IR spectrum (Figure 2) that presented the peak of borate functional group at 1226.85 cm^{-1} , 757.74 cm^{-1} and 721.89 cm^{-1} .

Cement characterization

1. Compressive strength of Cement

Compressive strength of 20BHA cement after mixed the various concentration of citric acid were determined by Universal Testing Machine, showed in Figure 3. The result is shown that the compressive strength increased gradually, the concentration of citric acid increased.

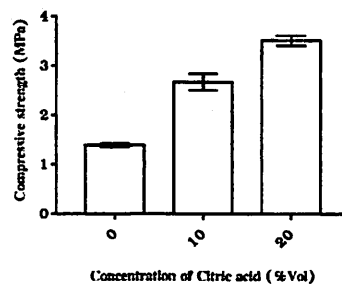


Figure 3 Compressive strength of the 20BHA with different concentration of citric acid after 21 days of setting

2. Morphology of 20BHA cement

The observation the morphological properties of 20BHA samples were investigated by SEM. From the Figure 4 (a) – (c), showed the microstructure of 20BHA with 0, 10 and 20% citric acid after 21 days, respectively. The particles size of 20BHA plates-like are decreased with the increase the citric concentration. These is results in the influence of citric acid that inhibit the 20BHA particles growth. (Tenhuisen & Brown, 1994).

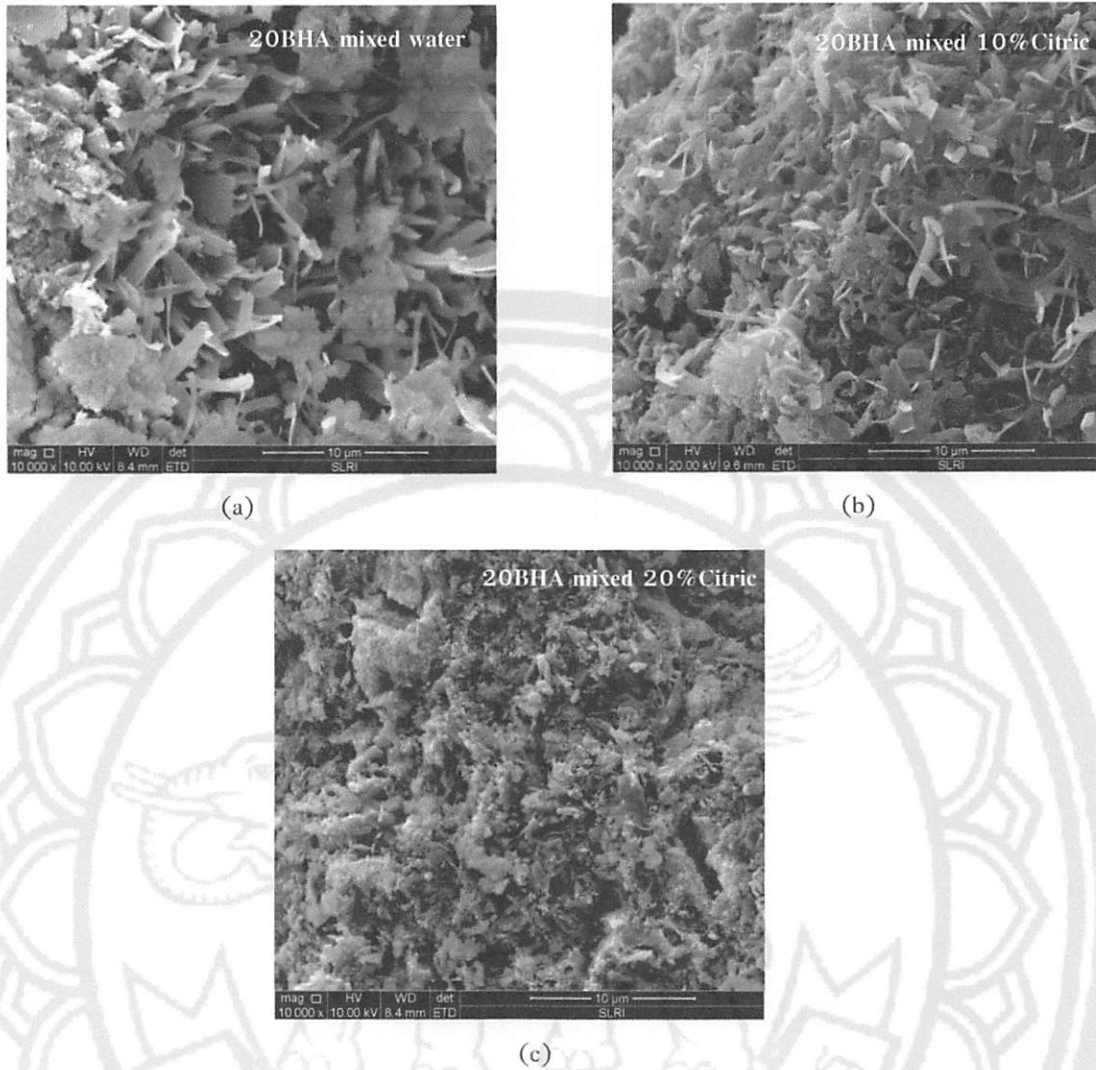


Figure 4 The SEM images of 20BHA with (a) 0%wt citric acid, (b) 10%wt citric acid and 20%wt citric acid after 21 days of setting

3. Phase analysis

The XRD results of the 20BHA with 0, 10 and 20% citric acid are shown in Figure 5. The 20BHA with 0%, 10% and 20% citric acid after 21 days setting have the XRD patterns similar to synthetic HA (JCPDS No. 74-0565). The crystallinity ($\%X_c$) can be calculated from XRD pattern, the data is given to Table 2. The concentration of citric acid has influence to 20BHA's crystallinity ($\%X_c$). These results also suggest that the concentration of citric acid are increase which leads to increase in the $\%X_c$. The results are in accord with the compressive strength results.

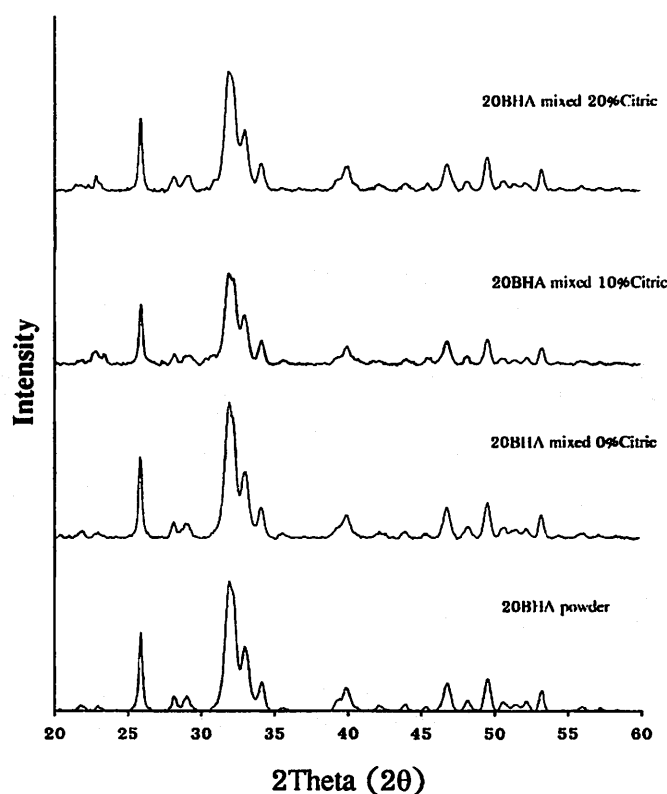


Figure 6 XRD patterns of the 2OBHA with different concentration of citric acid after 21 days of setting.

Table 2 Crystallinity (% X_c) of 2OBHA with different concentration of citric acid after 21 days of setting.

Samples Name	Crystallinity (% X_c)
2OBHA powder	55.42
2OBHA with 0% Citric acid	67.08
2OBHA with 10% Citric acid	70.13
2OBHA with 20% Citric acid	75.69

Discussion

This work performed to test the boron substitution into HA structure could be synthesized by wet chemical method at low temperature without control atmosphere that can be confirmed by XRD and FT-IR results. The XRD result showing the 2OBHA has a structure similar to synthetic HA. From the low-temperature synthesis condition can be occurred the CO_3 contamination into HA structure (Anwar, Asghar, Kanwal, Kazmi, & Sadiqa, 2016) which indicated the carbonyl group are shown in FT-IR result.

From the XRD and FT-IR results of 2OBHA powder are shown successfully substituted boron (B) into the HA structure, so the chemical formula would be $\text{Ca}_{10}(\text{PO}_4)_{4.8-x}(\text{CO}_3)_x(\text{BO}_3)_{1.2}(\text{OH})_2$.

The concentration of citric acid appeared affect to compressive strength and morphology of 2OBHA cement, it could be demonstrated by citric acid has inhibited the 2OBHA particles growth as showed in SEM image (Figure 4). SEM images confirmed the particle size of 2OBHA are decreased with increased citric acid concentration. The calculation of % X_c indicated that when increasing the level of the citric acid concentration



has a significantly effect to %X_c. However, some area for additional research are apparent from work presented in this research that would be interesting in the further experimental.

Conclusion

20BHA was synthesized via the co-precipitate method and preparation proceeded successfully that can be confirmed by XRD and FT-IR. However, the atmosphere has affected to the carbonated contamination of HA structure. In addition, 20BHA sample contains the boron in the form of borate (BO₃³⁻) ions and replace by PO₄³⁻ group. The crystalline of HA decreased when among of boron increased. The SEM results can be confirmed both of XRD and compressive strength results. Citric acid has a significant effect on the compressive strength properties of cement.

Acknowledgements

The authors would like to thank Department of materials engineering, Naresuan University Thailand for financial support and all this work.

References

- Ambard, A. J., & Mueninghoff, L. (2006). Calcium phosphate cement: Review of mechanical and biological properties. *Journal of Prosthodontics*, 15(5), 321–328. <https://doi.org/10.1111/j.1532-849X.2006.00129.x>
- Anwar, A., Asghar, M. N., Kanwal, Q., Kazmi, M., & Sadiqa, A. (2016). Low temperature synthesis and characterization of carbonated hydroxyapatite nanocrystals. *Journal of Molecular Structure*, 1117, 283–286. <https://doi.org/10.1016/j.molstruc.2016.03.061>
- Arora, M. (2013). Polymethylmethacrylate bone cements and additives: A review of the literature. *World Journal of Orthopedics*, 4(2), 67–74. <https://doi.org/10.5312/wjo.v4.i2.67>
- Cullity, B. D. (1978). Elements of X-ray diffraction. *American Journal of Physics*, 25(6), 394. <https://doi.org/10.1119/1.1934486>
- Fleet, M. E. (2009). Infrared spectra of carbonate apatites: V 2-Region bands. *Biomaterials*, 30(8), 1473–1481. <https://doi.org/10.1016/j.biomaterials.2008.12.007>
- Ginebra, M. P. (2009). *Cements as bone repair materials*. Technical University of Catalonia (UPC), Spain. Retrieved from <https://doi.org/10.1533/9781845696610.2.271>
- Kolmas, J., Velard, F., Jaguszewska, A., Lemaire, F., Kerdjoudj, H., Gangloff, S. C., & Kafalak, A. (2017). Substitution of strontium and boron into hydroxyapatite crystals: Effect on physicochemical properties and biocompatibility with human Wharton-Jelly stem cells. *Materials Science and Engineering: C*, 79, 638–646. <https://doi.org/10.1016/J.MSEC.2017.05.066>
- Landi, E., Tampieri, A., Celotti, G., & Sprio, S. (2000). Densification behaviour and mechanisms of synthetic hydroxyapatites. *Journal of the European Ceramic Society*, 20(14–15), 2377–2387. [https://doi.org/10.1016/S0955-2219\(00\)00154-0](https://doi.org/10.1016/S0955-2219(00)00154-0)



- Larsson, S., & Fazzalari, N. L. (2014). Anti-osteoporosis therapy and fracture healing. *Archives of Orthopaedic and Trauma Surgery*, 134(2), 291–297. <https://doi.org/10.1007/s00402-012-1558-8>
- Magnan, B., Bondi, M., Maluta, T., Samaila, E., Schirru, L., & Dall'Oca, C. (2013). Acrylic bone cement: Current concept review. *Musculoskeletal Surgery*, 97(2), 93–100. <https://doi.org/10.1007/s12306-013-0293-9>
- Nabiyouni, M., Ren, Y., & Bhaduri, S. B. (2015). Magnesium substitution in the structure of orthopedic nanoparticles: A comparison between amorphous magnesium phosphates, calcium magnesium phosphates, and hydroxyapatites. *Materials Science and Engineering C*, 52, 11–17. <https://doi.org/10.1016/j.msec.2015.03.032>
- Pan, Y., & Fleet, M. E. (2002). Compositions of the Apatite-Group Minerals: Substitution Mechanisms and Controlling Factors. *Reviews in Mineralogy and Geochemistry*, 48(1), 13–49. <https://doi.org/10.2138/rmg.2002.48.2>
- Pattanayak, D. K., Divya, P., Upadhyay, S., Prasad, R. C., Rao, B. T., & Rama Mohan, T. R. (2005). Synthesis and evaluation of hydroxyapatite ceramics. *Trends in Biomaterials and Artificial Organs*, 18(2), 87–92.
- Ratnayake, J. T. B., Mucalo, M., & Dias, G. J. (2017). Substituted hydroxyapatites for bone regeneration: A review of current trends. *Journal of Biomedical Materials Research - Part B Applied Biomaterials*, 105(5), 1285–1299. <https://doi.org/10.1002/jbm.b.33651>
- Safronova, T. V., Putlyaev, V. I., Shekhirev, M. A., Tretyakov, Y. D., Kuznetsov, A. V., & Belyakov, A. V. (2009). Densification additives for hydroxyapatite ceramics. *Journal of the European Ceramic Society*, 29(10), 1925–1932. <https://doi.org/10.1016/j.jeurceramsoc.2008.12.012>
- Sun, Y., Kwok, Y. C., & Nguyen, N. T. (2006). Low-pressure, high-temperature thermal bonding of polymeric microfluidic devices and their applications for electrophoretic separation. *Journal of Micromechanics and Microengineering*, 16(8), 1681–1688. <https://doi.org/10.1088/0960-1317/16/8/033>
- Šupová, M. (2015). Substituted hydroxyapatites for biomedical applications: A review. *Ceramics International*, 41(8), 9203–9231. <https://doi.org/10.1016/j.ceramint.2015.03.316>
- Tenhuisen, K. S., & Brown, P. W. (1994). The effects of citric and acetic acids on the formation of calcium-deficient hydroxyapatite at 38 °C. *Journal of Materials Science: Materials in Medicine*, 5(5), 291–298. <https://doi.org/10.1007/BF00122399>
- Ternane, R., Cohen-Adad, M. T., Panczer, G., Goutaudier, C., Kbir-Arighuib, N., Trabelsi-Ayedi, M., ... Massiot, D. (2002). Introduction of boron in hydroxyapatite: Synthesis and structural characterization. *Journal of Alloys and Compounds*, 333(1–2), 62–71. [https://doi.org/10.1016/S0925-8388\(01\)01558-4](https://doi.org/10.1016/S0925-8388(01)01558-4)
- Xu, H. H. K., Wang, P., Wang, L., Bao, C., Chen, Q., Weir, M. D., ... Reynolds, M. A. (2017). Calcium phosphate cements for bone engineering and their biological properties. *Bone Research*, 5, 17056. <https://doi.org/10.1038/boneres.2017.56>



- Yılmaz, B., & Evis, Z. (2016). Boron-Substituted Bioceramics: A Review. *Journal of Boron*, 1(1), 6–14. Retrieved from <http://journal.boren.gov.tr/article/view/5000176079>
- Zhang, W., Shen, Y., Pan, H., Lin, K., Liu, X., Darvell, B. W., ... Huang, W. (2011). Effects of strontium in modified biomaterials. *Acta Biomaterialia*, 7(2), 800–808. <https://doi.org/10.1016/j.actbio.2010.08.031>